Indonesian Physical Review
Volume 9 Issue 02, May 2026
P-ISSN: 2615-1278, E-ISSN: 2614-7904

The Effect of Deposition Temperature on Cu_2ZnSnS_4 (CZTS) Thin Films Grown by DC Magnetron Sputtering

Fianti[1*], Shila Artha Mulia[1], Nabila Rizkina Sari[1], Siti Firdhosiyah[1], Budi Astuti[1], Putut Marwoto[1], Kyoo Ho Kim[2], Muhammad Ikhlasul Amal[3], Ersan Yudhapratama Muslih[4]

[1] *Physics Department, Semarang State University, Semarang, Indonesia*
[2] *School of Materials Science and Engineering, Yeungnam University, Gyeongsan 712-749, Korea*
[3] *Research Center for Metallurgy and Materials, Indonesian Institute of Science, Serpong, Indonesia*
[4] *Mechanical Engineering, Trisakti University, Jakarta Barat, Indonesia*

Corresponding Author E-mail: fianti@mail.unnes.ac.id

Article Info

Article info:
Received: 27-10-2025
Revised: 14-02-2026
Accepted: 22-02-2026

Keywords:
thin films; Cu_2ZnSnS_4; DC Magnetron Sputtering; temperature

How To Cite:
Fianti, S. A. Mulia, N. R. Sari, S. Firdhosiyah, B. Astuti, P. Marwoto, K. H. Kim, M. I. Amal, E.Y. Muslih, "The Effect of Deposition Temperature on Cu_2ZnSnS_4 (CZTS) Thin Films Grown by DC Magnetron Sputtering", Indonesian Physical Review, vol. 9, no. 2, p 159- 175, 2026.

DOI:
https://doi.org/10.29303/ipr.v9i2.616.

Abstract

Cu_2ZnSnS_4 thin films were successfully deposited on soda lime glass substrates using the DC Magnetron Sputtering method at a plasma power of 42 W, an argon gas pressure of 500 mTorr, and deposition temperatures ranging from 27 °C to 400 °C for 7 hours, using a Cu_2ZnSnS_4 target with 99% purity. The effect of varying temperatures was characterized by using X-ray Diffraction (XRD) to determine the film structure, Scanning Electron Microscopy with Energy Dispersive X-ray Spectroscopy (SEM-EDX) to analyze morphology and composition, and UV-Vis-NIR spectrophotometry to evaluate optical properties. Film composition showed non-stoichiometric characteristics, with elemental ranges of Cu (20.66–32.81) %, Zn (14.08–25.67) %, Sn (21.87–37.05) %, and S (25.42–31.22) %. All samples exhibited a Cu/(Zn+Sn) ratio of less than 1, indicating Cu-poor compositions typical of p-type semiconductors. XRD analysis revealed that the formation of the Cu_2ZnSnS_4 phase began at a deposition temperature of 100 °C, while stable kesterite Cu_2ZnSnS_4 crystals were obtained at 400 °C, corresponding to the (112) crystal plane. The absorption coefficients and band gap energies ranged from 10^4 to $10^5 cm^{-1}$ and from 1.34 to 2.175 eV, respectively, confirming the suitability of the films for solar cell applications. SEM observations indicated that higher deposition temperature promoted more successful grain growth. Overall, higher deposition temperatures yield better Cu_2ZnSnS_4 thin films.

Introduction

Solar cell technology requires layers that can absorb more solar radiation. To achieve high efficiency, highly ordered crystalline structures are needed. It enhances device performance

but simultaneously increases production costs. Consequently, recent developments have increasingly focused on thin-film solar cell technology [1]. Thin-film technology, such as Cadmium Telluride (CdTe) in commercial modules, achieves efficiencies of 7-10% and 22.1% in laboratory-scale devices [2]. In addition, an efficiency of 19.2% in commercial modules has been successfully achieved through numerous studies on Copper Indium Gallium Diselenide (CIGS) [3] and 23.6% [4, 5] in a laboratory scale. Moreover, tandem perovskite-CIGS double-junction cells have reached 29.9% efficiency on a laboratory scale [6]. However, the constituent materials of CdTe, such as cadmium (Cd), are toxic heavy metals [7], and CIGS, such as selenium (Se), pose toxicity risks in the atmosphere [8], soil [9], and our food chain [10]. In addition, a major challenge for gallium (Ga), tellurium (Te), and indium (In) is the scarcity of their natural resources. These factors contribute to high production costs and restrict the scalability of solar cell manufacturing based on these compositions [11, 12]. Moreover, both materials were considered environmentally unfriendly, prompting the need to develop safe absorber materials derived from widely available natural resources [13]. CIGS (Cu (In, Ga) (S, Se) $_2$) has been identified as a rare and difficult-to-obtain material, resulting in relatively higher costs compared to Cu_2ZnSnS_4 [14]. The Cu_2ZnSnS_4 semiconductor has a high natural abundance and favorable properties, making it an alternative to CdTe and CIGS [15].

Cu_2ZnSnS_4 and CIGS share similar properties due to the derivation of the chalcopyrite structure of CIGS, in which two group III atoms in the periodic table (In or Ga) were replaced by Zn and Sn atoms through isoelectronic substitution [16]. Cu_2ZnSnS_4 (Copper-Zinc-Tin-Sulfide) can be in kesterite or stanite structure, depending on the location of Cu and Zn at its tetragonal [17]. Cu_2ZnSnS_4 is a p-type absorber which lies within the ideal window for solar energy conversion, with an absorption coefficient exceeding 10^4 cm^{-1} and a direct band gap in the range of 1.4–1.5 eV [12].

The Cu_2ZnSnS_4 solar cell absorber layer was grown using several methods, including sputtering, electrodeposition, nanoparticle-based techniques, evaporation, spray pyrolysis, and sol-gel synthesis [18]. Sputtering demonstrated uniform and stable deposition results, making it effective for large-scale manufacturing of thin films [19]. The fabrication of CZTS thin films at a temperature of 500 °C using the RF magnetron sputtering method with a single-compound Cu_2ZnSnS_4 target was carried out by Zhao *et al*., achieving an efficiency of 1.87% [20]. Under a deposition pressure of 5 mTorr for 30 minutes, an efficiency of 3.74% was achieved; however, the absorber layer exhibited low thickness and poor crystallinity [21]. According to previous research, the formation of well-defined crystal structures required high-temperature annealing conditions of approximately 550 °C for about 1.5 hours. The limited formation of Cu_2ZnSnS_4 crystals indicated that both the annealing temperature and duration still needed to be optimized.

The deposition process using RF magnetron sputtering method with Cu_2ZnSnS_4 target operating at a temperature of 200 °C and a power of 80 W for 2 hours was carried out by Sharmin *et al*., EDX analysis revealed that the resulting Cu_2ZnSnS_4 samples without sulfurization contained high levels of Cu and S, but deficient in Zn and Sn. 200 °C is a low temperture in a Cu_2ZnSnS_4 formation so far, unfurnotely, the minimum temperature of Cu_2ZnSnS_4 formation has not been known until now. Moreover, a significant loss of SnS was

observed above 500 °C, leading to the formation of surface voids and disrupting the film's stoichiometry. UV-Vis spectrophotometry showed that the thin films exhibited a direct band gap of 1.47-1.51 eV [22].

Band gap energy is not directly related to the deposition temperature in absorber thin film preparation; however, it is strongly influenced by the temperature during the recombination process at light harvesting for electrical charging on solar cells [23] and directly related to the condition of lattice expansion in its crystalline [24]. In spite of deposition, the band gap energy of a semiconductor depends on the crystallinity of the thin film [25, 26]. Moreover, the crystal formation is highly dependent on the temperature during its formation [27]. The resulting band gap energy of the thin film is not directly a function of deposition temperature during solar cell absorber preparation, but is more strongly influenced by the film's structural formation (i.e., phase and morphology).

This study aimed to analyze the effect of deposition temperature on Cu_2ZnSnS_4 thin film properties by preparing the films in DC magnetron sputtering at varied temperatures (from room temperature to 400 °C to find the minimum temperature for Cu_2ZnSnS_4 formation. The study began with thin-film preparation and then proceeded to characterization. The Cu_2ZnSnS_4 thin films were characterized to analyze particle size and surface morphology using Scanning Electron Microscopy (SEM), while chemical composition was examined using Energy Dispersive X-ray Spectroscopy (EDX), and the crystal structure was determined using X-ray Diffraction (XRD). The optical band gap values were evaluated using UV-Vis-NIR spectrophotometry to assess the potential of the films as efficient solar cell absorber layers.

Experimental Method

This method of study consisted of 3 major steps: substrate preparation, thin-film deposition, and characterization. The following work on thin film preparation and characterization is presented in Figure 1.

The materials used in this study included a Cu_2ZnSnS_4 target with 99% purity produced by Advanced Engineering Material China, soda lime glass (SLG) substrates, silver paste, ethanol, acetone, argon gas, and oxygen gas. The equipment used included a glass cutter, tweezers, an ultrasonic cleaner, measuring cylinders, mortar paper, plastic clips, and a DC magnetron sputtering reactor system. Characterization of the product was performed using SEM-EDX, XRD, and UV-Vis-NIR spectrophotometry.

SLG was selected as the substrate because its smooth surface supported thin-film growth, its transparency facilitated UV-Vis optical characterization, and its mechanical strength endured the moderate sputtering temperature range. The SLG was cut into 1 cm × 1 cm pieces to ensure uniform sample dimensions and compatibility with sputtering. The SLG was ultrasonically cleaned with acetone to remove oil, grease, and fingerprints, followed by ethanol to remove dust and residues not dissolved by acetone. Each step lasted 15 minutes. Nitrogen spray was applied after ultrasonic cleaning to dry the SLG and prevent water stains and oxidation.

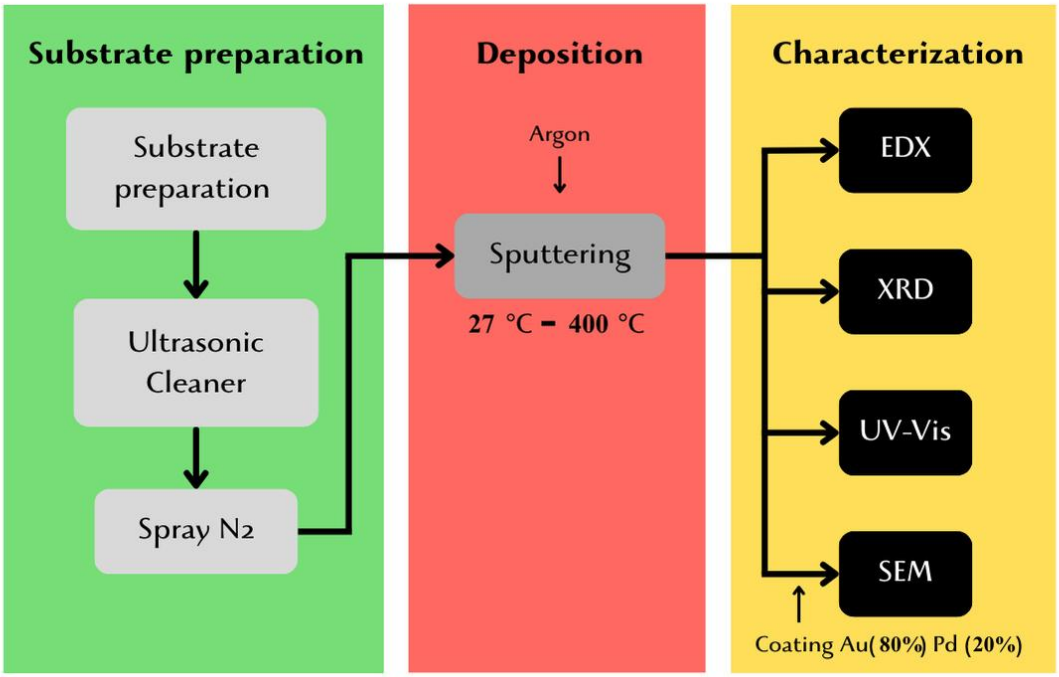

Figure 1. The flowing work of thin film preparation and charaterization.

The Cu_2ZnSnS_4 thin film deposition process began by opening the sputtering chamber, pressing the reset button, and setting the temperature to 27 °C to heat the anode, which helped glue the substrate to the anode. The Cu_2ZnSnS_4 target was placed on the cathode, and the soda-lime glass substrate was placed on the anode, both with silver paste adhesive. After the silver paste dried, the chamber was closed again. The vacuum pump was on, the temperature was set according to research parameters (27 °C, 100 °C, 200 °C, 300 °C, and 400 °C), and the temperature was monitored until it increased. The water pump was turned on, which functions as a magnetic cooler, and waited until it stabilized. Argon gas (99.999% purity) was flowed, and the pressure in the chamber was adjusted until stable at 500 mTorr. This gas pressure was maintained at ultra-high vacuum to ensure plasma stability. The power was set to 42 W for thin-film growth. The shutter was then opened, and the deposition process lasted 7 hours. After the deposition process was complete, the shutter was closed, the Argon flow was terminated, and the cooling heat treatment was complete.

SEM was used to characterize the surface morphology of Cu_2ZnSnS_4 thin films, providing information on homogeneity and crystal grain size [28]. Meanwhile, EDX was used to characterize the thin-film composition. The SEM-EDX characterization was conducted using a Hitachi SU 3500 SEM, and a maximum magnification of 300,000 times. Imaging was performed on two regions of the film surface at magnifications of 2,500 and 10,000, and the film was coated with Au (80%) and Pd (20%). The operating voltage used during SEM-EDX analysis was 10 kV.

XRD was used to identify the crystallographic plane indices and structural characteristics of a material through X-ray scattering [29]. A Panalytical X'Pert Powder diffractometer configured with a CuKα monochromator, a thin-film collimator, a fixed incident angle of 2°, and a wavelength of λ = 1.5406 Å was used to characterize the thin films. Measurements were conducted every 0.4 seconds under operating conditions of 40 kV and 30 mA, with a scan rate of 2° for each film. Diffraction data were collected over a 2θ range of 10° to 60 °.

The band gap was determined using UV-Vis-NIR spectroscopy under atmospheric pressure and temperature. In characterization, the transmittance of thin films was analyzed within a wavelength range of 300 nm to 1000 nm.

Result and Discussion

Chemical Composition of Cu_2ZnSnS_4 Thin Films

The resulting properties of the thin film are a function of the structural formation of Cu_2ZnSnS_4. Here, various deposition temperature was used for crystallization. Previous research conducted heat treatment to form Cu_2ZnSnS_4 at 500 °C for 1.5 hours [20] and formation from a quaternary target was needed at 200 °C for 2 hours [22]. Other research showed that Cu_2ZnSnS_4 started to form at 200 °C by spray deposition [30] at 50-60 °C for 60 min by chemical bath deposition [31], at 300 °C for 60 min in spray pyrolysis [32], at 300 °C for 60 min by single-step electrodeposition [33] and by spray deposition [34]. Besides, the formation of Cu_2ZnSnS_4 at lower than 200 °C has not been reported. Therefore, this research deposited Cu_2ZnSnS_4 thin films on SLG substrates using DC magnetron sputtering with a Cu_2ZnSnS_4 target at deposition temperatures ranging from room temperature to 400 °C. Moreover, this study used DC Magnetron Sputtering for optimal thin film solar cell absorber preparation with a lower power of 42 W and longer treatment of 7 hours than that of Zhao, 70 W [20] and Sharmin et al. of 80 W [22]. Lower power and longer interval times were used to achieve optimal grain growth, homogeneous morphology, and optimal crystal formation.

The chemical composition of Cu_2ZnSnS_4 thin films is presented in Figure 2. EDX characterization revealed the existence of Cu, Zn, Sn, and S elements in thin films, indicating that the Cu_2ZnSnS_4 was successfully coated on the SLG substrate using the DC magnetron sputtering method during the deposition process.

The atomic percentage composition of Cu_2ZnSnS_4 thin films was presented in Table 1. The variation in temperature triggers a relatively constant sulfur composition and a relative increase in Zn composition. It agreed with the result of Swami *et al.*, increasing the deposition temperature tended to increase the concentrations of zinc [30]. Based on Table 1, it was observed that tin (Sn) was the most dominant element in the Cu_2ZnSnS_4 thin films, followed by sulfur (S), copper (Cu), and zinc (Zn) was the least abundant. Xie *et al.* reported that the reduction in Zn content occurred during the single-ceramic sputtering process [35]. This reduction was attributed to evaporation during sputtering, as Zn possesses a high saturated vapor pressure. Additionally, elevated temperatures caused Zn to escape from the Cu_2ZnSnS_4 film composition.

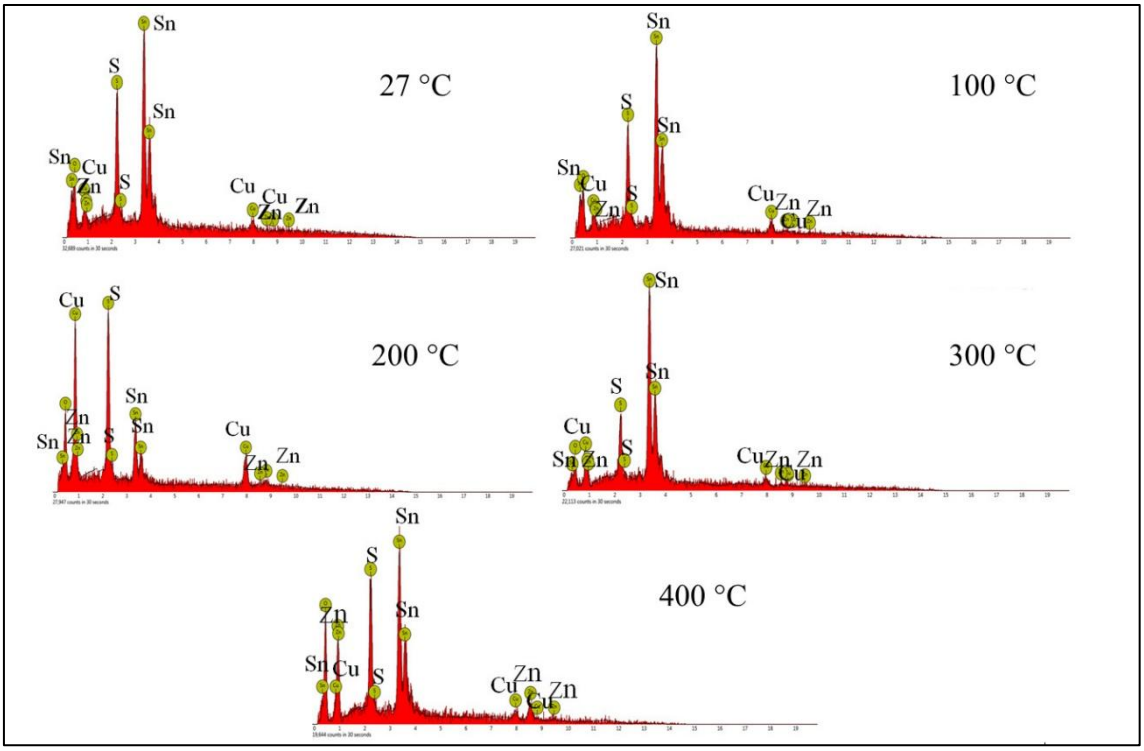

Figure 2. Chemical composition of Cu_2ZnSnS_4 thin films.

Table 1. Atomic percentage composition of Cu_2ZnSnS_4 thin films.

Deposition Temperature (°C)	Percentage Composition (%)				(Zn/Sn)	(Cu/(Zn+Sn))
	Cu	Zn	Sn	S		
27	20.90	16.79	37.05	26.28	0.45	0.39
100	20.66	17.32	36.59	25.42	0.47	0.38
200	32.81	14.08	21.87	31.22	0.64	0.91
300	24.79	14.62	34.76	25.78	0.42	0.50
400	20.16	25.67	26.49	27.68	0.96	0.39

The chemical composition of Sn showed sharp fluctuations at 200 °C, followed by an increase at 300 °C and another decrease at 400 °C. The excess Sn content was expected to contribute to the formation of a secondary SnS phase, although no SnS peaks were detected in the XRD spectra [36], According to Piacente *et al*., the evaporation of the sulfide compound SnS led to the loss of Sn [37], as in chemical reaction (1).

$$2SnS_2(s) \rightarrow Sn_2S_3(s) + \tfrac{1}{2}S_2(g) \rightarrow 2SnS(g) + \tfrac{1}{2}S_2(g) \quad (1)$$

Based on the chemical reaction (1), there is a potential for Sn loss when one of the Sn–S phases is formed. The absence of $S_2(g)$ or sulfur, such as H_2S, combined with low pressure, significantly accelerates the rate of Sn reduction. In this study, the loss of Sn composition occurred due to low sulfurization pressure or sulfurization carried out under ambient atmospheric pressure, along with the absence of elemental sulfur [38].

All samples in this study exhibited a Cu/(Zn+Sn) ratio is less than 1, indicating Cu-poor compositions, which classified the films as p-type semiconductors [39]. It was recognized that the absorber layer's chemical composition was a critical factor that could significantly affect a solar cell's performance. CZTS solar cells with high efficiency generally possess absorber layers with Zn-enriched and C-deficient compositions [40 - 43]. In this study, Zn-enriched and C-deficient characteristics were observed in films deposited at temperatures of 27 °C, 100 °C, and 400 °C, with Cu/(Zn+Sn) and Zn/Sn ratios of (0.39 and 0.45), (0.38 and 0.47), and (0.39 and 0.96), respectively. The optimal ratios for Cu/(Zn+Sn) and Zn/Sn were approximately 0.8 and 1.2, respectively [44]. The secondary phases that emerged due to the irregular growth of Cu_2ZnSnS_4 films made it difficult to determine or even to balance the stoichiometry [39].

The Structure of Cu_2ZnSnS_4 Thin Films

The X-ray diffraction graph of Cu_2ZnSnS_4 thin film is shown in Figure 3. Based on the diffractogram, the Cu_2ZnSnS_4 thin film deposited at 27 °C exhibited no diffraction peaks, indicating that the film has an amorphous structure. The Cu_2ZnSnS_4 thin film deposited at 100 °C showed three main diffraction peaks at 2θ = 28.77°, 34.00°, and 51.93°, corresponding to the (112), (202)/(020), and (301) crystal planes. Film deposited at 200 °C exhibited three primary peaks at 2θ = 28.81°, 29.98°, and 56.46°, which matched the (112), (103), and (312)/ (116) planes. The film deposited at 400 °C displayed six prominent diffraction peaks at 2θ = 28.79°, 29.78°, 34.08°, 47.71°, 51.83°, and 56.49°, corresponding to the (112), (103), (202)/ (020), (220)/ (204), (301), and (312)/ (116) planes. The crystalline nature of the Cu_2ZnSnS_4 thin films was confirmed by the presence of the diffraction peaks. The XRD patterns indicated that the films deposited at 100 °C, 200 °C, and 400 °C exhibited a kesterite structure of Cu_2ZnSnS_4, consistent with the COD database entry [96-900-4751]. Conversely, the film deposited at 300 °C showed several major peaks, but did not match the kesterite Cu_2ZnSnS_4 structure according to COD data. Therefore, the XRD pattern of the film deposited at 300 °C was shown separately from the others because it could not be compared with them (Figure 3).

According to Prashant *et al*., a dominant orientation along the (112) plane identified that Cu_2ZnSnS_4 predominantly exhibits a kesterite crystal structure [45]. The result was agreed, that in this study, the Cu_2ZnSnS_4 thin film deposited at 400 °C showed the highest peak intensity on the (112) plane compared to films deposited at 27 °C, 100 °C, 200 °C, and 300 °C.

The secondary phases were identified when weak diffraction peaks that did not correspond to the kesterite Cu_2ZnSnS_4 phase were observed [46]. These secondary phases may include Cu_2S, CuS, SnS, SnS_2, and ZnS [18]. In this study, the detected secondary phases were CuS (COD [96.101.0921]), ZnS (COD [96.101.1196], [96.2310816]), SnS (COD [96.810.251]), and SnS_2 (COD [96.703.8073]). The emergence of secondary phases in Cu_2ZnSnS_4 materials may lead to structural inconsistencies [47] and degrade solar cell performance [48]. According of Sun *et al*., the presence of Cu_xS impurity phases at temperatures between 350 °C and 400 °C suggested a notable rise in the copper fraction within the film [49].

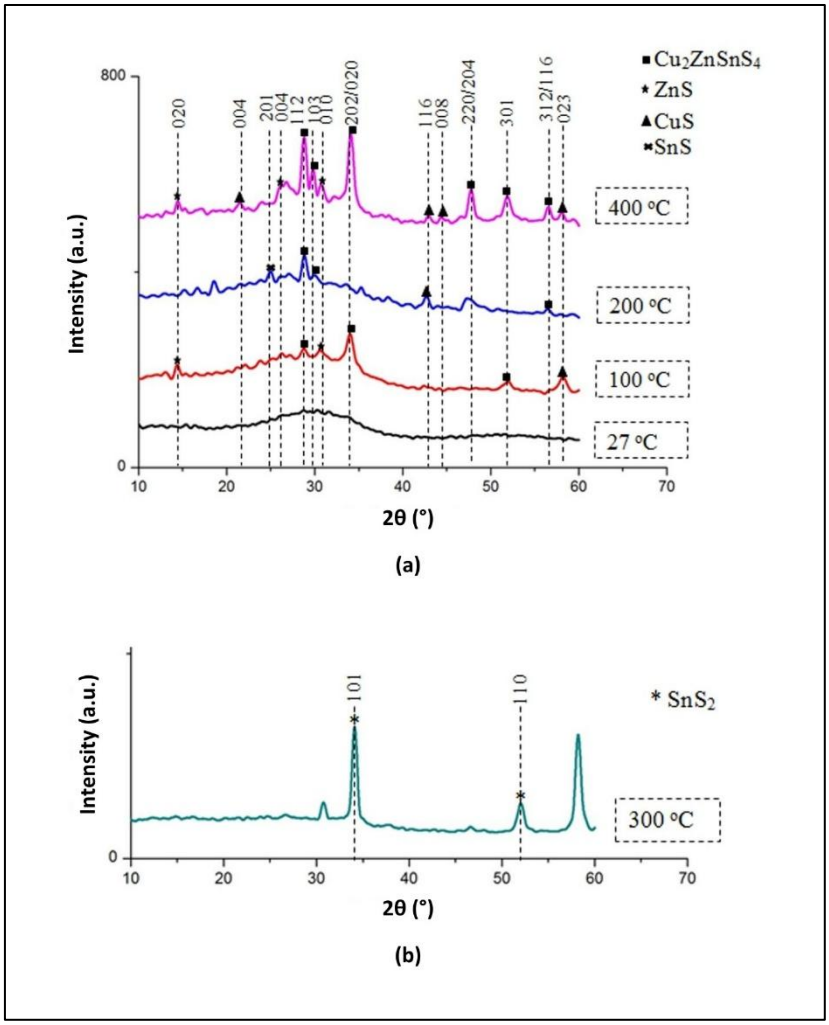

Figure 3. Film XRD graph of Cu_2ZnSnS_4 thin films (a) deposited at 27 °C, 100 °C, 200 °C, 400 °C, and (b) 300 °C.

The growth of p-type Cu_2ZnSnS_4 thin-film crystals through sputtering was successfully achieved by controlling pre-annealing parameters, followed by a sulfurization process [40]. According to Tang *et al.*, the formation of impurity phases was suppressed when a stoichiometric balance was achieved. At annealing temperatures within 500 °C and 550 °C, the CuxS impurity phase was not found, indicating that the ratio of Cu_2ZnSnS_4 had reached an ideal stoichiometric condition [50].

Table 2. Crystallite size calculation of Cu_2ZnSnS_4 thin films at the (112) peak.

Deposition Temperature (°C)	K	λ	FWHM / β (°)	β (rad)	θ	Cos θ	D (nm)
27	0.9	1.5406	-	-	-	-	-
100	0.9	1.5406	0.76	0.013264	14.385	0.968648	107.91
200	0.9	1.5406	0.59	0.010297	14.405	0.968561	139.02
300	0.9	1.5406	-	-	-	-	-
400	0.9	1.5406	0.46	0.008029	14.395	0.968605	178.29

Increasing the crystal's deposition temperature decreased the full width at half maximum (FWHM), as shown in Table 2. It was agreed by Sugianto *et al*. that the reported increase in deposition temperature led to a decrease in FWHM values [51]. Higher deposition temperatures allowed surface atoms on the substrate to become more homogeneous, adopt a more uniform orientation, and move more stably, thereby improving the crystalline quality of the films. Based on crystal structure analysis, FWHM values, and crystallite size, this study confirmed that the film deposited at 400 °C exhibited superior crystal quality compared to films deposited at 27 °C, 100 °C, 200 °C, and 300 °C (Table 2).

Optical Properties of Cu_2ZnSnS_4 Thin Films

The UV-Vis-NIR transmittance spectra are shown in Figure 4. It illustrated the comparative transmittance values of Cu_2ZnSnS_4 thin films grown on SLG substrates. The band gap energy of thin films deposited at 27-400 °C was evaluated from transmittance spectra.

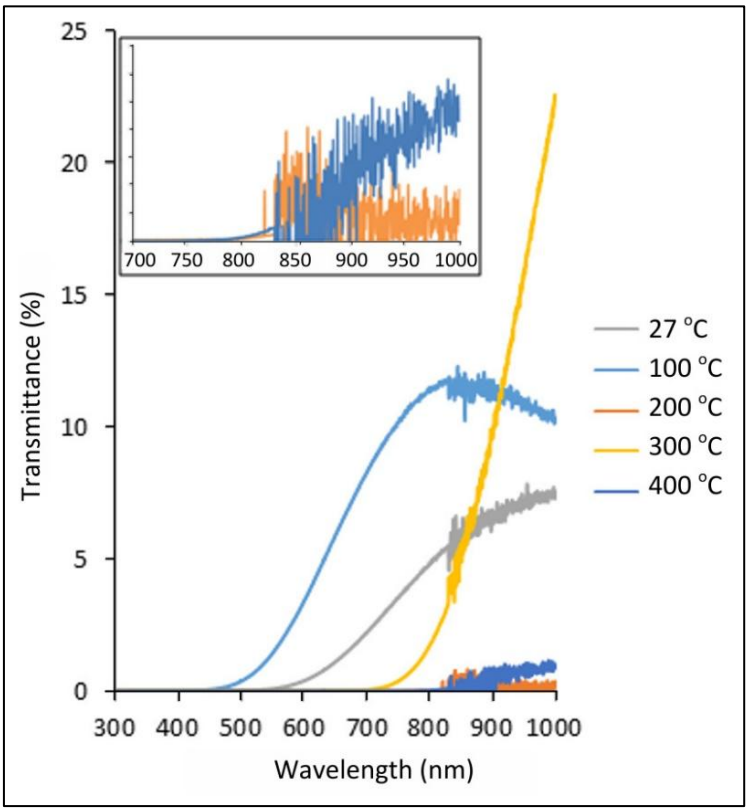

Figure 4. Transmittance spectra of Cu_2ZnSnS_4 thin films at a temperature range of 27 °C and 400 °C.

As shown in Figure 4, each film exhibited a distinct transmittance spectrum. In the region of fundamental transmission, where photons were absorbed by electrons transitioning from the valence band to the conduction band, maximum absorbance was observed in the visible light wavelength range at approximately 450 nm, 570 nm, and 720 nm for films deposited at 27 °C, 100 °C, and 300 °C, respectively. These three films showed significant changes in their transmission curves. In contrast, films deposited at 200 °C and 400 °C showed smaller changes in transmission curves, with maximum absorbance around 800 nm. The transmittance values

recorded for films deposited at 27 °C, 100 °C, 200 °C, 300 °C, and 400 °C were approximately 3.35915%, 0.01%, 0.066%, 0.0146%, and 0.15%, respectively. Several samples showed a decrease in the slope of the transmission curve, attributed to crystal defects that distorted the band [52].

The thin film's absorption coefficient was calculated from the slope of a correlation between transmittance and photon energy at each wavelength. The absorption coefficient values obtained from the Cu_2ZnSnS_4 thin-film samples were 5.26×10^4, 1.67×10^5, 1.17×10^4, 2.2×10^4, and 4.17×10^4 cm^{-1}, respectively. These were high absorption coefficients suitable for solar cell applications. This is according to the literature, the absorption coefficients and wavelength range of semiconductor absorber materials typically exhibit in the range of 10^4–10^5 cm^{-1} and 350–1000 nm [53].

Further, the thin film's absorption coefficient was used to evaluate the band gap using the Tauc Plot method (equation 2). The notation A is a constant of an arbitrary slope value, α is the absorption coefficient of the thin film, and hv is the photon energy. Eg is the energy separation between the bottom of the conduction band and the top of the valence band (or the band gap energy), and the value of n has been a constant corresponding to the probability of band-to-band transition, where $n = \frac{1}{2}$ for direct transition and $n = 2$ for indirect transition. Here, kesterite is in direct transition; thus, the ordinate of the y-axis in equation (2) was $(\alpha hv)^2$. The Tauc Plot method displayed the values of $(\alpha hv)^2$ as the ordinate and hv as the abscissa. Finally, band gap energy is determined by drawing a tangent line to the curve. When it decreases rapidly, the linear part of the graph of $(\alpha hv)^2$ versus hv. The intersection with the x-axis is the band gap energy (Eg). Tangent line plotting of Cu_2ZnSnS_4 thin-film on graphics of $(\alpha hv)^2$ versus hv can be seen in Figure 5. The tangent line was plotted at the rapid decrease of $(\alpha hv)^2$ showing the transition energy turning point.

$$(\alpha hv)^{\frac{1}{n}} = A(hv - Eg) \quad (2)$$

Table 3 shows the band gap energy and absorption coefficient of the Cu_2ZnSnS_4 thin films. As discussed before, the crystalline phase formed started at 100 °C, and structural characterization excluded the film deposited at 300 oC, so the discussion of optical Cu_2ZnSnS_4 focused on the films deposited at 100 °C, 200 °C, and 400 °C. The optimal Cu_2ZnSnS_4 semiconductor exhibits 1.4-1.6 eV [12, 22, 54]. According to films deposited at 100 °C (2.18 eV), 200 °C (1.3 eV), and 400 °C (1.44 eV), the band gap energy was decreasing in general. The XRD pattern shows that the crystallinity of Cu_2ZnSnS_4 increased with increasing temperature, as evidenced by the higher intensity of the (112) diffraction peak. The CuS secondary phase effect (having a wide band gap, 0.13 eV to 3.4 eV [55] and 1.38 eV to 1.82 eV [56] supported in lower band gap energy of 200 °C (1.3 eV) compared to 400 °C (1.44 eV), where the (116) Cu_2ZnSnS_4 was high enough that it overlapped with the CuS phase. Thus, generally, the grown thin films were suitable for solar cell absorber in the band gap energy and absorption coefficient point of view [41].

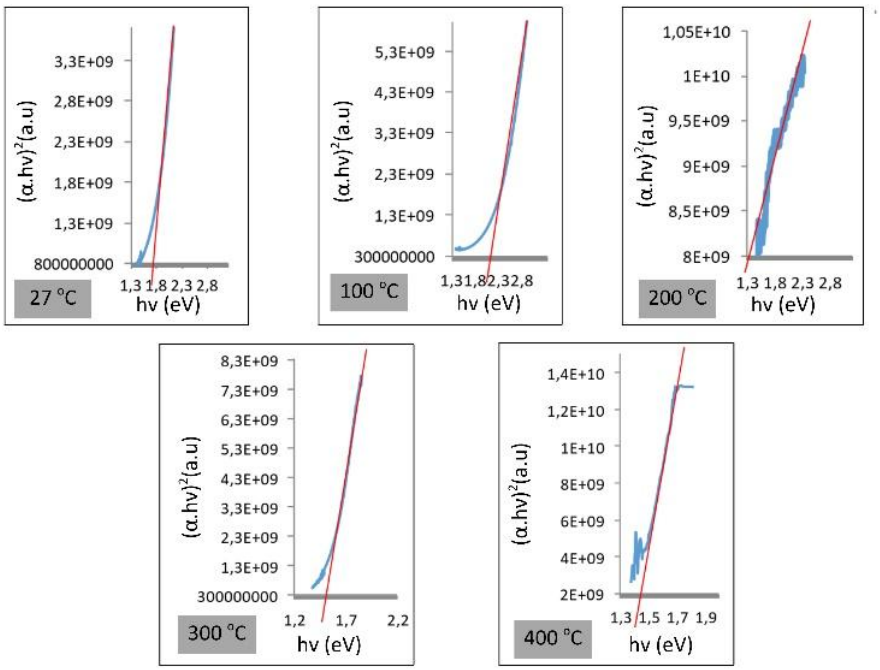

Figure 5. Band gap energy extrapolation of Cu_2ZnSnS_4 thin films deposited in the range of 27 °C and 400 °C

Table 3. The band gap energy (Eg) and absorption coefficient (α) of Cu_2ZnSnS_4 thin films

Deposition Temperature (°C)	Eg (eV)	α (cm^{-1})
27	1.765	5.26×10^4
100	2.175	1.67×10^5
200	1.34	1.17×10^4
300	1.545	2.22×10^4
400	1.435	4.17×10^4

Morphological Structure of Cu_2ZnSnS_4 Thin Films

Morphology of Cu_2ZnSnS_4 thin films deposited in the range of 27 °C and 400 °C is shown in Figure 6. The SEM result showed the morphology of the thin film at magnifications of 2,500 times or 10,000 times; all films exhibited uneven surface structures. The thin films deposited at 27 °C did not show any observable grain size, which was consistent with the XRD results, which indicated that the film deposited at 27 °C did not reveal any crystalline properties.

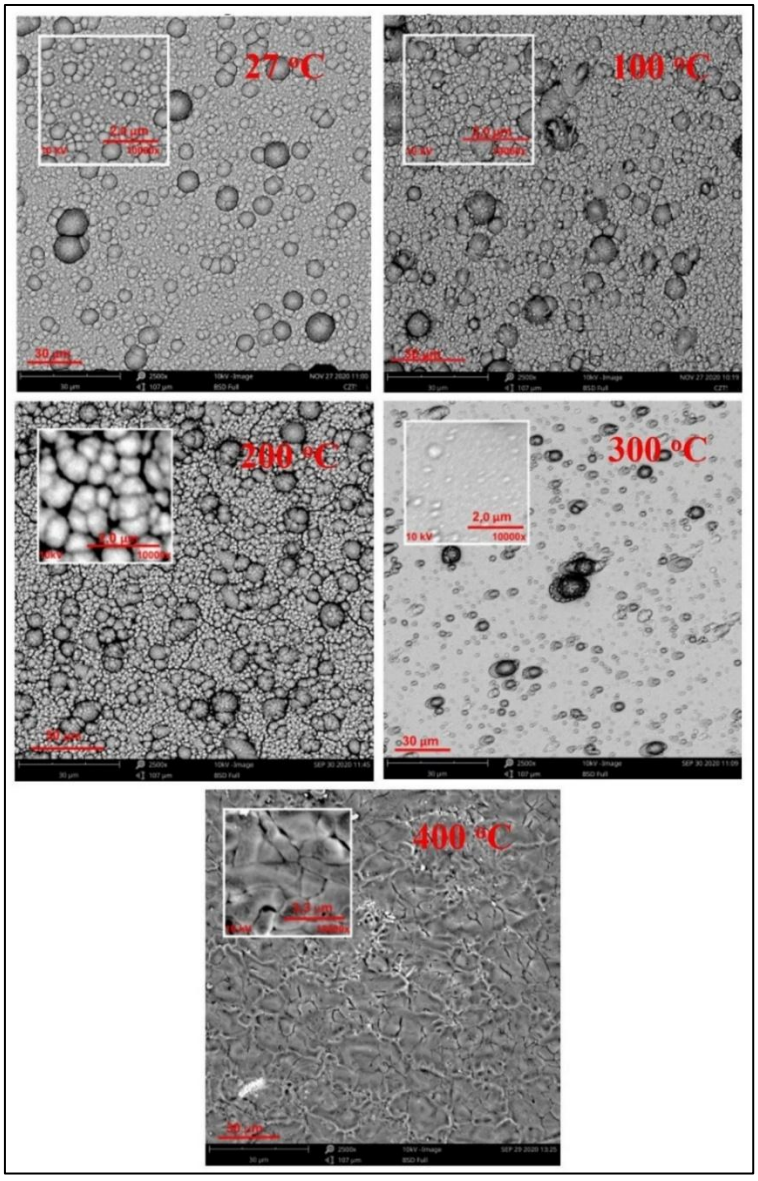

Figure 6. Morphology of Cu_2ZnSnS_4 thin films deposited in the range of 27 °C and 400 °C

The thin film deposited at 200 °C, observed at 2,500 times magnification, exhibited dense and non-uniform grains. At 10,000 times magnification, the grain structure appeared inhomogeneous, with small formations scattered across the surface and a spherical structure at the center of the image identified as a micro zinc flower [57]. The thin film deposited at 400 °C showed dense, compact grain growth and a homogeneous morphology at 2,500× magnification. It can be seen in detail at 10,000 times magnification.

The variation in surface morphology of the Cu_2ZnSnS_4 thin films was influenced by the deposition temperature, with the target sputtered, the thin film deposited onto the substrate, and the crystal grown simultaneously. The morphology and grain formation of Cu-based films grown via DC magnetron sputtering were primarily affected by power, working pressure, and

deposition time. The film's compactness was likely due to the annealing process following deposition [58]. Higher annealing temperatures tended to promote the formation of larger grain sizes [13].

Conclusion

The Cu_2ZnSnS_4 thin films were successfully grown by DC Magnetron Sputtering with temperature variation, i.e., 27 °C, 100 °C, 200 °C, 300 °C, and 400 °C. In addition, the elemental composition of Cu, Zn, Sn, and S in the Cu_2ZnSnS_4 thin films was found to be non-stoichiometric, with a Cu-poor ratio, and the films were classified as p-type semiconductors. Among these films, the closest to the standard composition of Cu_2ZnSnS_4 thin film was the film deposited at 200 °C. It revealed that Cu_2ZnSnS_4 film deposition can be handled in this temperature.

XRD analysis showed that the Cu_2ZnSnS_4 phase can be grown starting at 100 °C, and the Cu_2ZnSnS_4 phase grows optimally at 400 °C. Further, the secondary phases rose started at 300 °C. Optical characterization using UV-Vis-NIR spectrophotometry showed that all thin films showed a high absorption coefficient of 10^4–10^5 cm-1 and a varied band gap energy of 1.34-2.175 eV, which is suitable for a solar cell absorber. The data showed that higher deposition temperatures led to lower band gap energies in the films.

SEM observations showed that grain growth was greater at higher deposition temperatures, with the most compact and homogeneous grain structure observed in the film deposited at 400 °C. According to all characterization, the deposition temperature affected the properties of Cu_2ZnSnS_4 thin films, with the most suitable properties for a solar cell absorber observed for films grown at 400 °C.

Acknowledgment

The authors are thankful to the Faculty of Mathematics and Science of Universitas Negeri Semarang for the research fund under DPA number DPA 023.17.2.690645/2024.04/2024, in accordance with the agreement on faculty research 2024, number 196.28.3/UN37/PPK.04/2024.

References

[1] M. P. Suryawanshi *et al.*, "CZTS-based thin film solar cells: A status review," Mar. 2013.

[2] A. M. P. Abdul, K. Adhi, G. I. Aldhiantoro, D. R. Dewi, M. H. A. Baarik, and C. V. Anghel, "Cadmium telluride (CdTe) thin-film photovoltaics: A sustainable energy solution to support national energy resilience," *International Journal of Applied Mathematics, Sciences, and Technology for National Defense*, vol. 3, no. 2, pp. 77–88, 2025.

[3] A. Ravilla, E. Gullickson, A. Tomes, and I. Celik, "Economic and environmental sustainability of copper indium gallium selenide (CIGS) solar panels recycling," *Science of the Total Environment*, vol. 951, Nov. 2024.

[4] J. Keller *et al.*, "High-concentration silver alloying and steep back-contact gallium grading enabling copper indium gallium selenide solar cell with 23.6% efficiency," *Nat. Energy*, vol. 9, no. 4, pp. 467–478, Apr. 2024.

[5] NREL, "Best Research-Cell Efficiencies Chart," 2025. Accessed: Mar. 10, 2025. [Online]. Available: NREL. https ://www.nrel.gov/pv/cell-efficiency.html

[6] J. Ramanujam and U. P. Singh, "Copper indium gallium selenide-based solar cells – a review," *Energy Environ. Sci.*, vol. 10, no. 6, pp. 1306–1319, 2017.

[7] L. Wen, T. Zhu, T. Zhang, L. Li, and M. Ren, "Multi-omics and physiological traits analysis revealed the regulatory mechanism of selenium reducing cadmium toxicity in Desmodesmus abundans," *Ecotoxicol. Environ. Saf.*, vol. 303, Sep.

[8] M. A. Medinsky, R. G. Cuddihy, W. C. Griffith, S. H. Weissman, and R. O. McClellan, "Projected uptake and toxicity of selenium compounds from the environment," *Environ. Res.*, vol. 36, no. 1, pp. 181–192, 1985.

[9] R. Loomba *et al.*, "Exposure to a high selenium environment in Punjab, India: Effects on blood chemistry," *Science of the Total Environment*, vol. 716, May 2020.

[10] M. Banerjee, D. Chakravarty, P. Kalwani, and A. Ballal, "Voyage of selenium from environment to life: Beneficial or toxic?" *J. Biochem. Mol. Toxicol.*, vol. 36, no. 11, Nov. 2022.

[11] F. A. Jhuma, M. Z. Shaily, and M. J. Rashid, "Towards high-efficiency CZTS solar cell through buffer layer optimization," *Mater. Renew. Sustain. Energy*, vol. 8, no. 1, Mar. 2019.

[12] A. Benami, "Effect of CZTS Parameters on Photovoltaic Solar Cell from Numerical Simulation," *Journal of Energy and Power Engineering*, vol. 13, no. 1, pp. 32–36, Jan. 2019.

[13] L. Chen and C. Park, "Effects of annealing temperature on Cu_2ZnSnS_4 (CZTS) films formed by electrospray technique," *Korean Journal of Chemical Engineering*, vol. 34, no. 4, pp. 1187–1191, Apr. 2017.

[14] M. Haghighi, M. Minbashi, N. Taghavinia, D. H. Kim, S. M. Mahdavi, and A. A. Kordbacheh, "A modeling study on utilizing SnS_2 as the buffer layer of CZT (S, Se) solar cells," *Solar Energy*, vol. 167, pp. 165–171, Jun. 2018.

[15] S. Zhuk, A. Kushwaha, T. K. S. Wong, S. Masudy-Panah, A. Smirnov, and G. K. Dalapati, "Critical review on sputter-deposited Cu_2ZnSnS_4 (CZTS) based thin film photovoltaic technology focusing on device architecture and absorber quality on the solar cells performance," *Solar Energy Materials and Solar Cells*, vol. 171, pp. 239–252, Nov. 2017.

[16] S. Yazici *et al.*, "Growth of Cu_2ZnSnS_4 absorber layer on flexible metallic substrates for thin film solar cell applications," *Thin Solid Films*, vol. 589, pp. 563–573, Aug. 2015.

[17] M. Nishiwaki *et al.*, "Tail state formation in solar cell materials: First principles analyses of zincblende, chalcopyrite, kesterite, and hybrid perovskite crystals," *Phys. Rev. Mater.*, vol. 2, no. 8, pp. 1–28, Aug. 2018.

[18] J. H. Kim, "Developing Inorganic Thin Film Solar Cells using Earth-Abundant $Cu_2ZnSn(S, Se)_4$ Absorber Materials based on Sputtering Process," 2018.

[19] M. Yang, Z. Jiang, Z. Li, S. Liu, Y. Lu, and S. Wang, "Effects of different precursors on Cu_2ZnSnS_4 thin film solar cells prepared by sputtering method," *Mater. Sci. Semicond. Process*, vol. 56, pp. 238–242, Dec. 2016.

[20] Q. Zhao *et al.*, "Fabrication and characterization of Cu_2ZnSnS_4 thin films by sputtering a single target at different temperatures," *Physica B Condens. Matter*, vol. 523, pp. 62–66, Oct. 2017.

[21] H. Cui, X. Liu, L. Sun, F. Liu, C. Yan, and X. Hao, "Fabrication of efficient Cu_2ZnSnS_4 solar cells by sputtering single stoichiometric target," *Coatings*, vol. 7, no. 2, Feb. 2017.

[22] A. Sharmin, M. S. Bashar, M. Sultana, and S. M. M. Al Mamun, "Sputtered single-phase kesterite Cu_2ZnSnS_4 (CZTS) thin film for photovoltaic applications: Post annealing parameter optimization and property analysis," *AIP Adv.*, vol. 10, no. 1, Jan. 2020.

[23] Y. P. Varshni, "Temperature dependence of the energy gap in semiconductors," *Physica*, vol. 34, no. 1, pp. 149–154, 1967.

[24] Y. Zhang, Z. Wang, J. Xi, and J. Yang, "Temperature-dependent band gaps in several semiconductors: from the role of electron–phonon renormalization," *Journal of Physics: Condensed Matter*, vol. 32, no. 47, p. 475503, 2020.

[25] B. Mbaluka John, S. W. Mugo, and J. M. Ngaruiya, "Dependence of Optical Band Gap on Crystallite Size of TiO2 Thin Films Prepared using Sol Gel Process," *European Journal of Material Science*, vol. 8, no. 1, pp. 1–12, 2021.

[26] S. Benramache, O. Belahssen, A. Guettaf, and A. Arif, "Correlation between crystallite size–optical gap energy and precursor molarities of ZnO thin films," *Journal of Semiconductors*, vol. 35, no. 4, Apr. 2014.

[27] K. Deng *et al.*, "Temperature Dependence on Microstructure, Crystallization Orientation, and Piezoelectric Properties of ZnO Films," *Sensors*, vol. 25, no. 1, 2025.

[28] E. S. Hassan, A. N. Abd, and M. O. Dawood, "The Sputter Time Duration Effect on the Structural and Optical Properties of Zinc Oxide by RF Magnetron Sputtering," *Silicon*, vol. 10, no. 6, pp. 2901–2906, Nov. 2018.

[29] S. Rahman, "Rancangan Eksperimen Analisis Struktur Mikro Sampel dengan Prinsip XRD Menggunakan Metode Kristal Berputar," *Jurnal Riset dan Kajian Pendidikan Fisika*, vol. 3, no. 1, pp. 5–9, 2016.

[30] S. K. Swami, N. Chaturvedi, A. Kumar, and V. Dutta, "Effect of deposition temperature on the structural and electrical properties of spray deposited kesterite (Cu_2ZnSnS_4) films," *Solar Energy*, vol. 122, pp. 508–516, Dec. 2015.

[31] R. Digraskar, K. Gattu, B. Sathe, A. Ghule, and R. Sharma, "Temperature-dependent fabrication of cost-effective and nontoxic Cu_2ZnSnS_4 (CZTS) thin films for solar cell," *AIP Conf. Proc.*, vol. 1728, no. 1, p. 020326, May 2016.

[32] F. Z. Boutebakh, N. Attaf, and M. S. Aida, "Effect of growth temperature on the physical properties of kesterite Cu_2ZnSnS_4 (CZTS) thin films," *Discov. Mater.*, vol. 5, no. 1, Dec. 2025.

[33] M. H. Rashid *et al.*, "Characterization of single-step electrodeposited Cu_2ZnSnS_4 thin films," *Journal of Optics (India)*, vol. 47, no. 3, pp. 256–262, Sep. 2018.

[34] S. A. Khalate, R. S. Kate, J. H. Kim, S. M. Pawar, and R. J. Deokate, "Effect of deposition temperature on the properties of Cu_2ZnSnS_4 (CZTS) thin films," *Superlattices Microstruct.*, vol. 103, pp. 335–342, Mar. 2017.

[35] M. Xie, D. Zhuang, M. Zhao, B. Li, M. Cao, and J. Song, "Fabrication of Cu_2ZnSnS_4 thin films using a ceramic quaternary target," *Vacuum*, vol. 101, pp. 146–150, 2014.

[36] S. A. Nadi *et al.*, "Postdeposition annealing effect on CunSnS thin films grown at different substrate temperatures," *International Journal of Photoenergy*, vol. 2014, 2014.

[37] V. Piacente, S. Foglia, and P. Scardala, "Sublimation study of the tin sulphides SnS2, Sn2S3 and SnS," *J. Alloys Compd.*, vol. 177, no. 1, pp. 17–30, 1991.

[38] J. Scragg, "PHD Studies of Cu_2ZnSnS_4 films prepared by sulfurisation of electrodeposited precursors," Thesis, University of Bath, 2010.

[39] K. Yu and E. A. Carter, "Determining and Controlling the Stoichiometry of Cu_2ZnSnS_4 Photovoltaics: The Physics and Its Implications," *American Chemical Society*, vol. 28, pp. 1–20, Jun. 2016.

[40] J. Jiang, L. Zhang, W. Wang, X. Huang, and R. Hong, "The role of pre-annealing in the sulfurization of Cu-Zn-Sn stacked metal layer prepared by magnetron sputtering," *Mater. Sci. Semicond. Process*, vol. 83, pp. 125–132, Aug. 2018.

[41] S. Siebentritt and S. Schorr, "Kesterites-a challenging material for solar cells," *Progress in Photovoltaics: Research and Applications*, vol. 20, no. 5, pp. 512–519, Aug. 2012.

[42] C. Malerba *et al.*, "Stoichiometry effect on Cu_2ZnSnS_4 thin films morphological and optical properties," *Journal of Renewable and Sustainable Energy*, vol. 6, no. 1, Jan. 2014.

[43] A. Ennaoui *et al.*, "Cu_2ZnSnS_4 thin film solar cells from electroplated precursors: Novel low-cost perspective," *Thin Solid Films*, vol. 517, no. 7, pp. 2511–2514, Feb. 2009.

[44] Q. Guo *et al.*, "Fabrication of 7.2% efficient CZTSSe solar cells using CZTS nanocrystals," *J. Am. Chem. Soc.*, vol. 132, no. 49, pp. 17384–17386, Dec. 2010.

[45] P. K. Sarswat, M. L. Free, and A. Tiwari, "Temperature-dependent study of the Raman A mode of Cu_2ZnSnS_4 thin films," *Phys. Status Solidi B Basic Res.*, vol. 248, no. 9, pp. 2170–2174, Sep. 2011.

[46] T. P. Dhakal, C. Y. Peng, R. Reid Tobias, R. Dasharathy, and C. R. Westgate, "Characterization of a CZTS thin film solar cell grown by sputtering method," *Solar Energy*, vol. 100, pp. 23–30, Feb. 2014.

[47] A. Aldalbahi, E. M. Mkawi, K. Ibrahim, and M. A. Farrukh, "Effect of sulfurization time on the properties of copper zinc tin sulfide thin films grown by electrochemical deposition," *Sci. Rep.*, vol. 6, Sep. 2016.

[48] C. J. Hages *et al.*, "Identifying the Real Minority Carrier Lifetime in Nonideal Semiconductors: A Case Study of Kesterite Materials," *Adv. Energy Mater.*, vol. 7, no. 18, Sep. 2017.

[49] L. Sun, J. He, H. Kong, F. Yue, P. Yang, and J. Chu, "Structure, composition and optical properties of Cu_2ZnSnS_4 thin films deposited by Pulsed Laser Deposition method," *Solar Energy Materials and Solar Cells*, vol. 95, no. 10, pp. 2907–2913, Oct. 2011.

[50] D. Tang *et al.*, "An alternative route towards low-cost Cu_2ZnSnS_4 thin film solar cells," *Surf. Coat. Technol.*, vol. 232, pp. 53–59, oct. 2013.

[51] Sugianto, P. Marwoto, B. Astuti, R. Zannah, and Yanti, "Pengaruh Temperatur Deposisi terhadap Struktur dan Sifat Optik Film Tipis ZnO: Al dengan metode DC Magnetron Sputtering," *Jurnal Fisika*, vol. 5, 2015.

[52] R. Moreno, E. A. Ramirez, and G. Gordillo Guzmán, "Study of optical and structural properties of CZTS thin films grown by co-evaporation and spray pyrolysis," in *Journal of Physics: Conference Series*, Institute of Physics Publishing, Feb. 2016.

[53] J. Poortmans and V. Arkhipov, "Thin Film Solar Cells Fabrication, Characterization and Applications," in *Thin Film Solar Cells*, J. Poortmans and V. Arkhipov, Eds., Wiley, 2006.

[54] S. M. Pawar *et al.*, "Single step electrosynthesis of Cu_2ZnSnS_4 (CZTS) thin films for solar cell application," *Electrochim. Acta*, vol. 55, no. 12, pp. 4057–4061, Apr. 2010.

[55] R. S. Christy, J. Thampi, and T. Kumaran, "Phase Transition in CuS Nanoparticles," *Journal of Non-Oxide Glasses*, vol. 6, no. 1, pp. 13–22, 2014.

[56] A. M. Abdulwahab *et al.*, "Synthesis, characterization, and anti-cancer activity evaluation of Ba-doped CuS nanostructures synthesized by the co-precipitation method," *The Royal Society of Chemistry Advances*, vol. 15, no. 6, pp. 4669–4680, Feb. 2025.

[57] E. Mkawi, K. Ibrahim, M. K. M Ali, and A. Salhin Mohamed, "Dependence of Copper Concentration on the Properties of Cu_2ZnSnS_4 Thin Films Prepared by Electrochemical Method," *Int. J. Electrochem. Sci.*, vol. 8, pp. 359–368, 2013.

[58] A. Khalkar, K. S. Lim, S. M. Yu, S. P. Patole, and J. B. Yoo, "Deposition of Cu_2ZnSnS_4 thin films by magnetron sputtering and subsequent sulphurization," *Electronic Materials Letters*, vol. 10, no. 1, pp. 43–49, Jan. 2014.